

A New Type of Uniformly Stacked Phase in Tetrathiapentalene-Based Organic Metals

Yoshimasa Bando, Takahiro Matsuzawa, Norihiro Takashita, Tadashi Kawamoto, Takehiko Mori,* and Jun-ichi Yamada[1]

Department of Organic and Polymeric Materials, Tokyo Institute of Technology, Ookayama 2-12-1, Meguro-ku, Tokyo 152-8552

[1]Department of Material Science, Graduate School of Material Science, University of Hyogo, 3-2-1 Kouto, Kamigori-cho, Ako-gun, Hyogo 678-1297

Received March 10, 2005; E-mail: takehiko@o.cc.titech.ac.jp

Two new organic electron donor molecules are synthesized on the basis of the ethylthio-substituted tetrathiapentalenes with a methylenedithio or a 1,3-dithiane unit. These donors provide four isostructural radical-cation salts, which belong to a new crystal type with uniform stacks of the donor molecules. These salts show metallic conductivity down to low temperatures, linear temperature dependence of the thermoelectric power, and asymmetrical ESR lineshapes. The obtained uniform structure is compared with the previous uniform structure from the viewpoint of crystal packing.

In the study of molecular conductors,[1] better control of molecular arrangements is an essential challenge for achieving desired conducting properties. A large variety of crystal structures can emerge from a single donor molecule in the radical-cation salts of BEDT-TTF (bis(ethylenedithio)tetrathiafulvalene).[2] As an attempt to design a donor molecule with an extended π-skeleton, in 1992 Misaki et al. prepared bis-fused TTF (tetrathiafulvalene) donors, which are called TTP (tetrathiapentalene) donors (Scheme 1).[3] An accumulation of structural data of TTP salts in the following decade has shown us that the crystal types of TTP salts are relatively limited, depending on the kind of the TTP molecules.[4] For example, the unsubstituted TTP molecule forms stacks with considerable two-dimensional interaction, tetrakis(methylthio)-TTP (TTM-TTP) provides highly one-dimensional columns, and bis(methylthio)ethylenedithio-TTP (TMET-TTP) gives a large number of θ-phase crystals. One drawback of TTP donors is, however, their low solubility. In order to increase the solubility of donor molecules, one must usually attach alkylthio substituents. In TTF donors, even the methylthio group of small bulk prohibits the intercolumnar interaction, so that no superconductor has been found based on the donors containing alkylthio groups. In addition, the ethylthio-substituted TTF does not give good crystals of the charge-transfer salts. We have, however, found that bis(ethylthio)ethylenedithio-TTP (C_2TET-TTP, Scheme 1) affords a series of charge-transfer salts having uniform donor stacks, which show metallic conductivity down to low temperatures.[5] The ethylthio groups are standing perpendicular to the molecular plane, and do not prohibit the transverse interactions between the donor columns. Therefore,

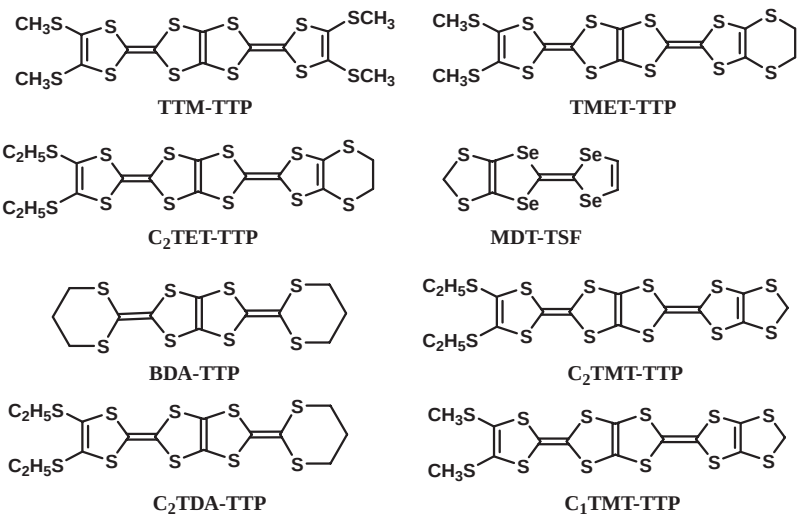

Scheme 1.

Published on the web August 4, 2005; DOI 10.1246/bcsj.78.1442

it is a good strategy to introduce the ethylthio groups in TTP donors to improve the solubility of TTP molecules while keeping the metallic two-dimensional band structure.

Recently, two new types of organic superconductors have been found. One type is the MDT-TSF (methylenedithiotetraselenafulvalene, Scheme 1) superconductors. The MDT-TSF donor constructs uniform columns with linear anions, and the donor columns and the anion columns are incommensurate, so that the resulting composition is like (MDT-TSF)-$(AuI_2)_{0.436}$.[6] Such compounds show superconductivity at 4–5 K. The other type is the BDA-TTP (2,5-bis(1,3-dithian-2-ylidene)-1,3,4,6-tetrathiapentalene, Scheme 1) superconductors. Although the BDA-TTP donor does not have a TTF skeleton and contains a TTP skeleton instead, many of its salts, such as β-$(BDA\text{-}TTP)_2PF_6$, show superconductivity.[7]

To explore changes of molecular packing patterns, in the present work, we have synthesized the ethylthio-substituted TTP with a methylenedithio unit (C_2TMT-TTP: 2-[4,5-bis-(ethylthio)-1,3-dithiol-2-ylidene]-5-(4,5-methylthio-1,3-dithiol-2-ylidene)-1,3,4,6-tetrathiapentalene, Scheme 1) or a 1,3-dithiane unit (C_2TDA-TTP: 2-[4,5-bis(ethylthio)-1,3-dithiol-2-ylidene]-5-(1,3-dithian-2-ylidene)-1,3,4,6-tetrathiapentalene, Scheme 1). Each appended unit is a component part of MDT-TSF or BDA-TTP, so C_2TMT-TTP is expected to decrease the steric effect, but C_2TDA-TTP is expected to increase it. However, both donors have provided the same new type of uniformly stacked phases, $(C_2TMT\text{-}TTP)_2PF_6$, $(C_2TMT\text{-}TTP)_2AuBr_2$, and $(C_2TDA\text{-}TTP)_2PF_6$. Interestingly, even the methylthio analog of C_2TMT-TTP, C_1TMT-TTP (2-(4,5-bis-(methylthio)-1,3-dithiol-2-ylidene)-5-(4,5-methylthio-1,3-dithiol-2-ylidene)-1,3,4,6-tetrathiapentalene, Scheme 1), which is a reported donor,[8] has provided the same crystal structure $(C_1TMT\text{-}TTP)_2PF_6$. In addition, C_2TDA-TTP has given several insulating phases such as $(C_2TDA\text{-}TTP)_2$(DMTCNQ) (DMTCNQ: 2,5-dimethyl-1,4-tetracyanoquinodimethane) and $(C_2TDA\text{-}TTP)GaCl_4$. This paper reports crystal structures and physical properties of these compounds.

Results

Synthesis. Scheme 2 outlines the synthesis of C_2TMT-TTP (**3**) and C_2TDA-TTP (**6**). C_2TMT-TTP (**3**) was prepared by the phosphite-mediated cross-coupling reaction of **1** and **2**.[3,8] Although analogous donors of C_2TDA-TTP (**6**) have been reported to be obtained by the cross-coupling reaction using **7**,[9] we examined an alternative synthetic route to **6** via the cross-coupling of **1** and **4**.[10] Compound **4** was prepared as follows: (i) the $Et_2O\cdot BF_3$-mediated reaction of 2,3-dichloro-1,4-dioxane with a tin derivative of 2-thiolo-1,3-dithiole-4,5-dithiolate;[11] (ii) the $Et_2O\cdot BF_3$-promoted skeletal rearrangement in the presence of 1,3-propanedithiol;[12] and (iii) conversion into the corresponding oxone by using mercury(II) acetate. Compound **4** reacted with **1** in toluene containing $(MeO)_3P$ at 110 °C to give the coupling product **5**. Subsequent DDQ (2.3-dichloro-5,6-dicyano-1,4-benzoquinone) oxidation of **5** in TCE (1,1,2-trichloroethane) led to C_2TDA-TTP (**6**) in 71% yield. It should be noted that changing the solvent used for the DDQ oxidation from TCE to toluene causes a low yield (3%) of **6**. Thus, we accomplished the synthesis of **6** by the use of **4** instead of **7**.

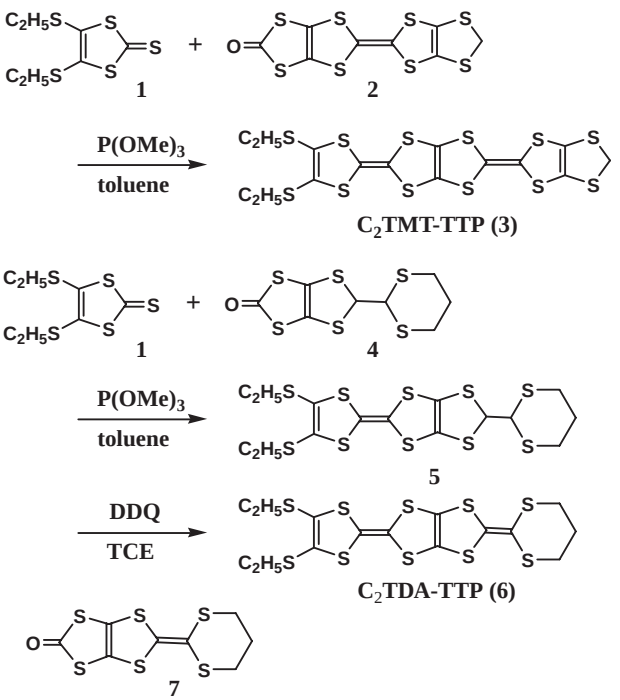

Scheme 2.

Table 1. Redox Potentials (V)[a)]

Compounds	E_1	E_2	E_3	E_4	$\lvert E_1 - E_2 \rvert$
C_1TMT-TTP	0.54	0.77	0.98	1.18	0.23
C_2TMT-TTP	0.50	0.73	0.92	1.14	0.23
TMET-TTP	0.53	0.74	1.00	1.18	0.21
C_2TET-TTP	0.49	0.73	0.99	1.23	0.24
C_2TDA-TTP	0.56	0.85	1.20		0.29
5	0.52	0.90			0.38
TTF	0.36	0.85			0.49
BEDT-TTF	0.50	0.85			0.35

a) vs Ag/AgCl in Bu_4NPF_6/PhCN.

Electrochemical Properties. The solution redox properties of the prepared donors are investigated by cyclic voltammetry. Table 1 summarizes their redox potentials together with those of related donors. The C_nTMT-TTP ($n = 1$ and 2) donors show four reversible redox couples up to 4+, corresponding to the oxidation of four 1,3-dithiole rings. The redox potentials are essentially the same as those of the ethylenedithio analogs, TMET-TTP and C_2TET-TTP. There is a tendency that the respective first oxidation potentials of the ethylthio compounds (C_2TMT-TTP and C_2TET-TTP) are lower by 0.04 V than those of the methylthio compounds (C_1TMT-TTP and TMET-TTP).

C_2TDA-TTP shows only three redox couples. It is therefore supposed that the 1,3-dithiane ring does not participate in the oxidation. This is also agreeable with the observation of only two redox couples in BDA-TTP.[7] Interestingly, the first oxidation potential of the synthetic intermediate **5** is by 0.04 V lower than that of the final donor, C_2TDA-TTP. Researches have suggested that the single-bonded 1,3-dithiane does not affect the redox properties,[10] so that the oxidation potential of **5** is basically the same as that of the corresponding methylthio-TTF. Thus, it is reasonable that the oxidation potentials of **5** are not

Table 2. Conditions of Electrochemical Oxidation of Crystal Growth

Donor	Anion	Solvent	Current/μA	Composition[a)]	Forms	σ_{rt}/S cm^{-1}
C_1TMT-TTP	PF_6	THF	0.5	2:1 (X)	Brown plate	500
C_2TMT-TTP	PF_6	THF	0.5	2:1 (X)	Black plate	500
	$AuBr_2$	PhCN	0.2	2:1 (X)	Black plate	600
	TCNQ	THF	Direct reaction	?	Brown plate	3 (T_{MI} = 30 K)
C_2TDA-TTP	PF_6	PhCl	0.5	2:1 (X)	Black plate	200
	PF_6	PhCl	1	1:1 (E)	Black needle	8×10^{-5}
	$GaCl_4$	PhCl	0.5	1:1 (X)	Black block	$<10^{-6}$
	$FeCl_4$	PhCl	0.5	1:1 (E)	Black block	2×10^{-3}
	SbF_6	PhCl	1	1:3 (E)	Black needle	4×10^{-2}
	DMTCNQ	THF	Direct reaction	2:1 (X)	Black needle	$<10^{-6}$

a) X determined from single crystal X-ray structure analysis, and E based on the energy dispersion spectroscopy (EDS) from the ratio of S and the central element of the anion.

Table 3. Crystallographic Data of C_nTMT-TTP Salts

	$(C_2TMT\text{-}TTP)_2PF_6$	$(C_1TMT\text{-}TTP)_2PF_6$	$(C_2TMT\text{-}TTP)_2AuBr_2$
Formula	$C_{30}H_{24}F_6PS_{24}$	$C_{26}H_{16}F_6PS_{24}$	$C_{30}H_{24}AuBr_2PS_{24}$
Formula weight	1299.07	1242.96	1510.87
Shape	Black plate	Brown plate	Black plate
Crystal system	Monoclinic	Monoclinic	Monoclinic
Space group	$C2/m$	$C2/m$	$C2/m$
a/Å	32.85(1)	33.44(1)	31.37(1)
b/Å	12.242(3)	12.083(2)	12.128(5)
c/Å	5.904(1)	5.9743(7)	5.924(2)
β/°	97.54(2)	99.55(1)	99.01(3)
V/Å^3	2354(1)	2380.3(8)	2226(1)
Z	2	2	2
D_{calc}/g cm^{-3}	1.833	1.734	2.254
R_1/R_w[a)]	0.048/0.174	0.077/0.271	
Reflections	3586	3629	

a) $R_1 = \Sigma||F_o| - |F_c||/\Sigma|F_o|$. $R_w = [\Sigma w(|F_o| - |F_c|)^2/\Sigma wF_o^2]^{1/2}$.

much different from those of BEDT-TTF. On the other hand, the oxidation potentials of BDA-TTP are higher by 0.16 V than those of the 1,3-dithiolane (five-membered ring) analog.[7] Accordingly, we conclude that the conjugated 1,3-dithiane unit considerably weakens the donor ability.

Crystal Growth. Charge transfer complexes were prepared by the electrochemical oxidation of the donors in the presence of tetrabutylammonium salts of various anions. The conditions of the prepared salts are listed in Table 2. Crystals of $(C_2TDA\text{-}TTP)_2$(DMTCNQ) were prepared by the direct reaction of the THF solutions of C_2TDA-TTP and DMTCNQ, followed by slow evaporation of the solvent at room temperature.

Crystal and Electronic Structures of $(C_1TMT\text{-}TTP)_2PF_6$, $(C_2TMT\text{-}TTP)_2PF_6$, $(C_2TMT\text{-}TTP)_2AuBr_2$, and $(C_2TDA\text{-}TTP)_2PF_6$. Crystallographic data of these salts are listed in Tables 3 and 4. Satisfactory structure analyses are carried out for two isostructural salts $(C_1TMT\text{-}TTP)_2PF_6$ and $(C_2TMT\text{-}TTP)_2PF_6$. $(C_2TMT\text{-}TTP)_2AuBr_2$ has almost the same lattice constants and is considered to have the same structure. $(C_2TDA\text{-}TTP)_2PF_6$ is also isostructural, although the quality of the structure analysis is not very good. The structures of the donor molecules are shown in Fig. 1. Since these salts are isostructural, the crystal structure is depicted for the C_2TMT-TTP salt (Fig. 2). A half of the donor molecule is crystallographically independent; the donor exists on a mirror plane perpendicular to the molecular plane. One quarter of the anion molecule is crystallographically independent because the PF_6 anion is located on a $2/m$ position. Accordingly the composition is 2:1. The donor molecules are uniformly stacked along the c axis (Fig. 2b).

The donor molecules are almost flat (Fig. 1a). The terminal ethyl groups extend almost perpendicular to the molecular plane. The perpendicular conformation is common to other ethylthio donors such as C_2TET-TTP,[5] whereas one of the methyl carbons in θ-type TMET-TTP salts extends to the side of the molecules, nearly within the molecular plane.[13] The perpendicular conformation of the present salts facilitates the intercolumnar interactions between the uniform columns. The donor columns interact with each other along the b axis (Fig. 2a), and the conducting sheets spread along the bc plane. The anions are located in the pocket sandwiched between the methylenedithio units (Fig. 2a). The outer methylene carbon is slightly deviated from the molecular plane; 0.79 Å for

Table 4. Crystallographic Data of C_2TDA-TTP Salts

	$(C_2TDA\text{-}TTP)_2PF_6$	$(C_2TDA\text{-}TTP)_2(DMTCNQ)$	$(C_2TDA\text{-}TTP)GaCl_4$
Formula	$C_{30}H_{32}F_6PS_{20}$	$C_{44}H_{40}N_4S_{20}$	$C_{15}H_{16}Cl_4GaS_{10}$
Formula weight	1178.87	1266.15	728.42
Shape	Black plate	Black plate	Black block
Crystal system	Monoclinic	Orthorhombic	Orthorhombic
Space group	$C2/m$	$Pbca$	
a/Å	32.769(8)	16.12(1)	9.253(4)
b/Å	12.445(3)	30.48(4)	18.342(9)
c/Å	5.711(6)	11.22(1)	18.046(7)
β/°	97.67(4)		
V/Å^3	2308(2)	5513(8)	3062(2)
Z	2	4	4
D_{calc}/g cm^{-3}	1.697	1.526	1.580
R_1/R_w[a)]	0.133/0.387	0.094/0.254	
Reflections	1540	8068	

a) $R_1 = \Sigma||F_o| - |F_c||/\Sigma|F_o|$. $R_w = [\Sigma w(|F_o| - |F_c|)^2/\Sigma wF_o^2]^{1/2}$.

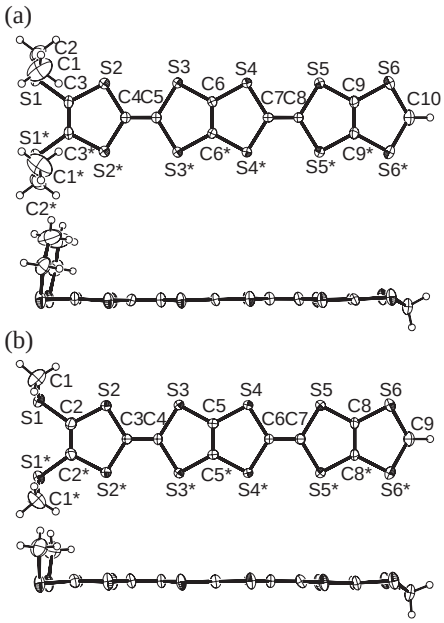

Fig. 1. (a) ORTEP drawing of top and side views of the donor molecule in $(C_2TMT\text{-}TTP)_2PF_6$, and the atomic numbering scheme. (b) ORTEP drawing of top and side views of the donor molecule in $(C_1TMT\text{-}TTP)_2PF_6$, and the atomic numbering scheme.

$(C_2TMT\text{-}TTP)_2PF_6$ and 0.55 Å for $(C_1TMT\text{-}TTP)_2PF_6$. Interplanar distances in the uniform columns are 3.48 Å, 3.51 Å, and 3.48 Å for $(C_2TMT\text{-}TTP)_2PF_6$, $(C_1TMT\text{-}TTP)_2PF_6$, and $(C_2TDA\text{-}TTP)_2PF_6$, respectively, and the slip distances along the donor long axes are 4.77 Å, 4.84 Å, and 4.54 Å. These values are almost the same as 3.47 Å and 4.72 Å in $(C_2TET\text{-}TTP)_2ClO_4$,[5] so that the structures of a single column are basically identical (Fig. 2d).

In order to investigate the electronic structure, we have calculated the intermolecular overlap integrals S_i between the highest occupied molecular orbitals (HOMOs) on the basis of the extended Hückel molecular orbital calculation (Table 5).[14] The sulfur 3d atomic orbitals are not included, because the calculation without S 3d gives the correct anisotropy in the case of stacked structures (β-type).[15] A similar calculation for $(C_2TET\text{-}TTP)_2ClO_4$ is also listed in Table 5. The interstack interaction p1 amounts to one-third or one-quarter of the intrastack interaction c, so that the two-dimensional interaction is considerable. The symmetry of $(C_2TET\text{-}TTP)_2ClO_4$ is lower, owing to the lack of a mirror plane, and there are four π interactions, but the anisotropy is almost the same for this compound.

The tight-binding band structure is calculated from the transfer integrals t_i estimated from $t_i = E \times S_i$, where the energy level of HOMO is $E = -10$ eV. As shown in Fig. 3, the Fermi surface of $(C_2TMT\text{-}TTP)_2PF_6$ is open but quite corrugated. The energy level at the Γ point is very close to the Fermi level, and if this energy level is below the Fermi level, the Fermi surface is closed. This happens sensitively depending on the parameters of the atomic orbitals, and the calculation including the sulfur 3d atomic orbital gives the closed Fermi surface.[5] Therefore the present compound and its isostructural $(C_1TMT\text{-}TTP)_2PF_6$ are located on the boundary between the quasi-one-dimensional electronic structure with the open Fermi surface and the two-dimensional one with the closed Fermi surface. The previous experiments for similarly stacked structures have suggested that the former is probably true.[15]

In addition to the uniform phase $(C_2TDA\text{-}TTP)_2PF_6$, C_2TDA-TTP affords another insulating 1:1 salt with the same anion, $(C_2TDA\text{-}TTP)PF_6$ (Table 2). These crystals are obtained in the same batch, but are easily distinguished from the crystal shapes.

Crystal Structure of $(C_2TDA\text{-}TTP)_2(DMTCNQ)$. Crystal data of $(C_2TDA\text{-}TTP)_2(DMTCNQ)$ are listed in Table 4. The crystal structure is depicted in Fig. 4. The crystal belongs to an orthorhombic space group, *Pbca*. One donor molecule is located on a general position, and the DMTCNQ molecule is on an inversion center. Consequently, the composition is 2:1. The donor and acceptor molecules construct DDA-type mixstacked columns along the c axis (Fig. 4b). The interplanar distances are 3.46 Å for D–D and 3.39 Å for D–A. In the stack, the long axis of DMTCNQ is not perfectly parallel to that of the donor molecule (about 7°), probably owing to the existence of the methyl groups (Fig. 4c). The donor molecule has a

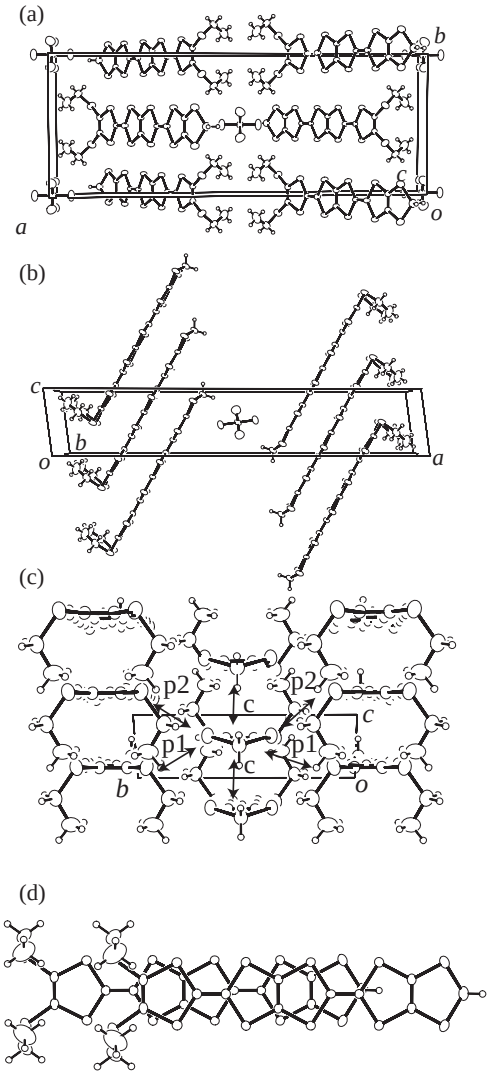

Fig. 2. Crystal structure of $(C_2TMT\text{-}TTP)_2PF_6$, (a) projection along the *c* axis, (b) projection along the molecular short axis, and (c) view along the donor long axis. (d) Overlap mode of the donor molecules.

Table 5. Intermolecular Overlap Integrals S_i ($\times 10^{-3}$) between HOMOs

	c	p1	p2	p3	p4
$(C_2TMT\text{-}TTP)_2PF_6$	10.1	−2.51	−0.64		
$(C_1TMT\text{-}TTP)_2PF_6$	9.32	−2.95	−0.43		
$(C_2TET\text{-}TTP)_2ClO_4$	10.2	−2.0	−0.63	−2.76	0.05

slightly bent structure, even at the 1,3-dithiole ring with the ethylthio parts. This indicates that the donor molecule is practically neutral; such a condition is consistent with the weak acceptor ability of DMTCNQ and the relatively weak donor ability of $C_2TDA\text{-}TTP$ (Table 2). The ethylthio parts are standing perpendicular to the molecular plane, and the outer half of the 1,3-dithiane ring is out of the molecular plane because the 1,3-dithiane ring has a chair-like conformation. Since this complex is composed of mixed stacks of neutral donors and acceptors, this complex is an insulator ($\sigma_{rt} < 10^{-6}$ S cm^{-1}).

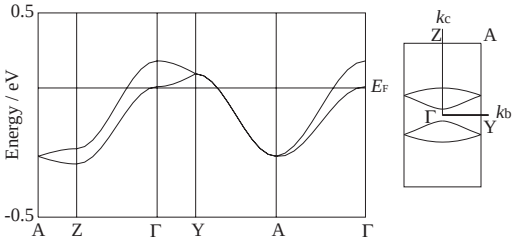

Fig. 3. Band structure and the Fermi surface of $(C_2TMT\text{-}TTP)_2PF_6$.

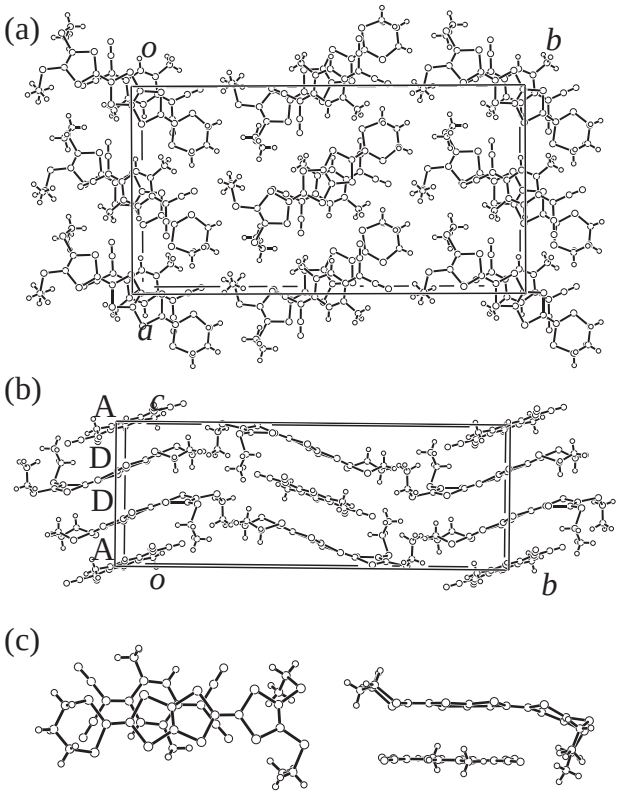

Fig. 4. Crystal structure of $(C_2TDA\text{-}TTP)_2(DMTCNQ)$, (a) projection along the *c* axis, and (b) projection along the *a* axis. (c) Overlap mode and side views of the donor and the acceptor.

Although the structure analysis of $(C_2TDA\text{-}TTP)GaCl_4$ is not completed, the preliminary structural investigation suggests that this is a 1:1 salt, and that the donors construct strongly dimerized one-dimensional columns along the *a* axis. In addition, there is a strong two-fold modulation along the *a* axis. Because this is a dimerized 1:1 salt, this complex is also an insulator ($\sigma_{rt} < 10^{-6}$ S cm^{-1}).

Transport Properties. As shown in Fig. 5a, the temperature dependence of the resistivity of the four isostructual salts shows metallic conductivity down to low temperatures, although the resistivity of $(C_2TDA\text{-}TTP)_2PF_6$ increases slightly below 15 K. In addition, $(C_2TDA\text{-}TTP)_2PF_6$ exhibits a lower electrical conductivity than the $C_nTMT\text{-}TTP$ salts ($n = 1, 2$): 200 S cm^{-1} for $(C_2TDA\text{-}TTP)_2PF_6$ in contrast to about 500 S cm^{-1} for the $C_nTMT\text{-}TTP$ salts. The $C_2TDA\text{-}TTP$ salt is not such a good metal as the other salts, probably because

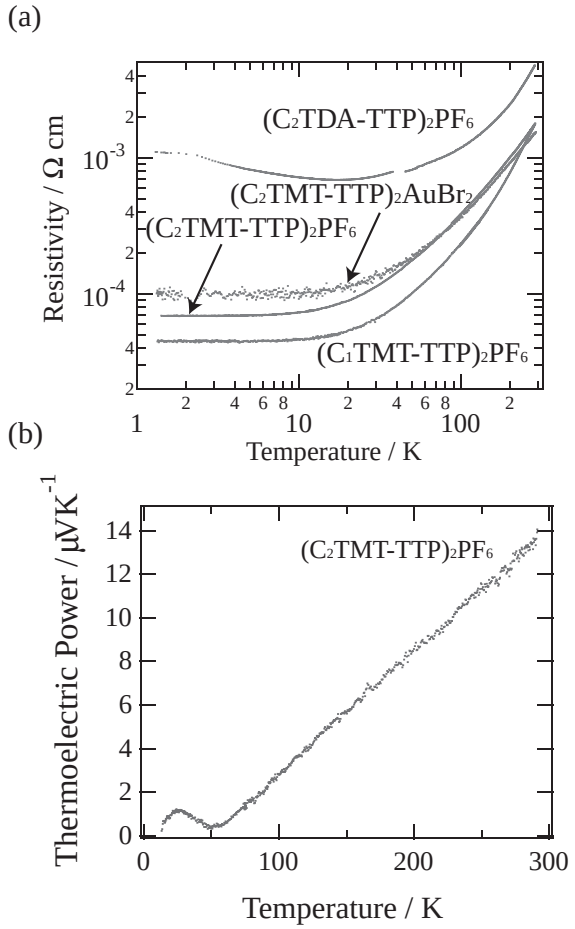

Fig. 5. Transport properties of $(C_n\text{TMT-TTP})_2X$ and $(C_2\text{TDA-TTP})_2PF_6$. (a) Electrical resistivity of $(C_n\text{TMT-TTP})_2X$ and $(C_2\text{TDA-TTP})_2PF_6$ and (b) thermoelectric power of $(C_2\text{TMT-TTP})_2PF_6$.

the out-of-plane 1,3-dithiane unit in C_2TDA-TTP may enhance the correlation effect.

Figure 5b shows the temperature dependence of the thermoelectric power of $(C_2\text{TMT-TTP})_2PF_6$. The thermoelectric power shows linear temperature dependence down to about 50 K, below which the thermoelectric power once increases and again decreases. The resulting peak around 25 K is probably associated with phonon drag.[16] Assuming the one-dimensional tight-binding band, one can estimate the bandwidth ($4t_c$) to be 1.2 eV from the high-temperature linear part. The bandwidth of $(C_2\text{TET-TTP})_2X$ (X = BF_4, ClO_4) is similarly obtained to be about 0.86 eV.[5] These results indicate that the bandwidth of the present C_2TMT-TTP salt is larger than those of the previous C_2TET-TTP salts, although the calculated intrastack overlap integrals are practically the same (Table 5).

Electron Spin Resonance. X-band ESR has been measured for $(C_2\text{TMT-TTP})_2PF_6$ (Fig. 6). At room temperature, we can observe a single Lorentzian, attributable to the electron spin located on the TTP donor, with $g = 2.0029$ and $\Delta H_{pp} =$ 17 G when the magnetic field is applied perpendicular to the molecular plane, and with $g = 2.0110$ and $\Delta H_{pp} = 23$ G when the magnetic field is parallel to the molecular long axis. Upon cooling, the linewidth decreases linearly (Fig. 7), and the spin

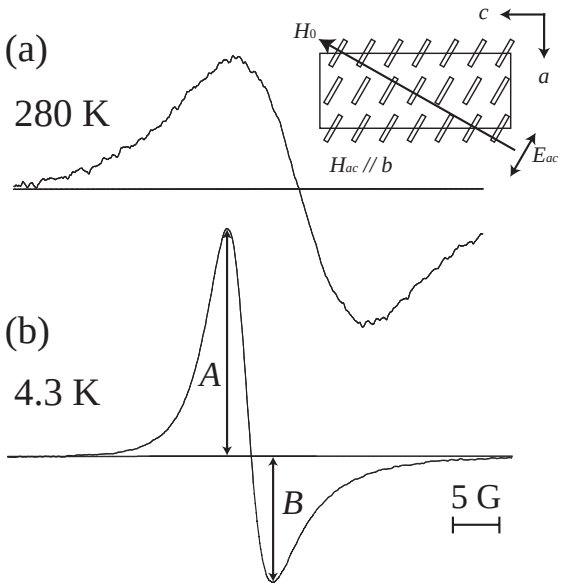

Fig. 6. Lineshape of ESR spectra in $(C_2\text{TMT-TTP})_2PF_6$ (a) at 280 K and (b) at 4.3 K. The inset in (a) shows the directions of the applied magnetic and microwave electric fields.

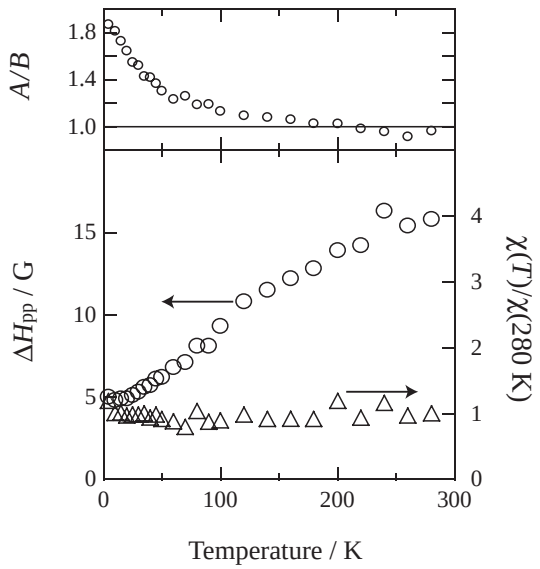

Fig. 7. Temperature dependence of the peak-to-peak linewidth ΔH_{pp} and the normalized spin susceptibility, and the A/B ratio between the maximum and minimum of the derivative of absorption for $(C_2\text{TMT-TTP})_2PF_6$ when the magnetic field is applied perpendicular to the molecular plane.

susceptibility remains almost constant, which is consistent with the Pauli-like paramagnetic properties in a good metal.

Below 100 K, the lineshape becomes rather asymmetrical; here the A/B ratio amounts to 1.9 at 4 K (Figs. 6 and 7). The present compound is located at the intermediate situation where the line shape is gradually converted to the Dysonian lineshape.[17,18] This is associated with the good metallic nature of the present compound at low temperatures.

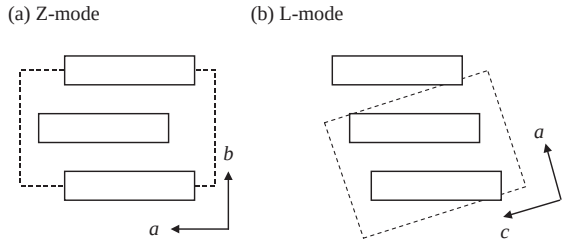

Fig. 8. Two different packing modes of uniform stacks, (a) Z-mode found in the present salts ($(C_2TMT\text{-}TTP)_2PF_6$) and (b) L-mode observed in $(C_2TET\text{-}TTP)_2ClO_4$, viewed along the donor columns.

Discussion

The structures of a single uniform column in the four salts: $(C_1TMT\text{-}TTP)_2PF_6$, $(C_2TMT\text{-}TTP)_2PF_6$, $(C_2TMT\text{-}TTP)_2AuBr_2$, and $(C_2TDA\text{-}TTP)_2PF_6$, described herein, are almost the same as those in the previous C_2TET-TTP salts: $(C_2TET\text{-}TTP)_2ClO_4$, and $(C_2TET\text{-}TTP)_2BF_4$.[5] Nonetheless, the lattice constants are entirely different; the former four salts have space group $C2/m$, and the latter two salts have $C2/c$, although both types of crystals belong to the monoclinic system. The stacking directions are, respectively, the c and b axes. In addition, the unit cell volumes of the former are about half of the latter type. These differences come from the column packings. As for the intercolmunar interactions like p1 and p2 (Fig. 2), the TTP part slips by half of the 1,3-dithiole unit (1.6 Å) from the neighboring donor. If the slip happens alternately in opposite directions, in a zig-zag manner (Fig. 8a), the columns are arranged ($\|b$) exactly perpendicular to the donor long axis. This is the case of the present four salts. If the slip occurs in the same direction, the conducting sheet spreads in the tilted direction ($\|a$ in Fig. 8b) from the donor long axis. This difference is the same as the distinction of the Z-mode (Zig-zag form) and L-mode (Linear form) observed in θ-type BEDT-TTF salts.[2] Thus the present crystals are regarded as having a Z-mode uniform-stack structure, which is a new structural type that is different from the L-mode uniform structure in the C_2TET-TTP salts.

There are further differences. In the neighboring conducting sheets along the a axis (Fig. 2b), the long axes of the donors are tilted in the same direction, whereas those in the C_2TET-TTP salts are tilted in opposite directions. The present Z-mode crystals have a mirror plane intercepting the molecular plane, so that the p1 and p2 interactions appear symmetrically (Fig. 2c), while the donor molecule in the L-mode crystals is located on a general position, and there are four π interactions. The existence of the mirror plane is related to the symmetrical donor structure of the methylenedithio unit. By contrast, two carbon atoms of an ethylenedithio unit are never on the same plane, and are never symmetrical, as a BEDT-TTF molecule seldom has an intercepting mirror plane. Accordingly, the Z-mode crystal is associated with a symmetrical donor molecule, while the L-mode crystal indicates possible deviation from the symmetrical structure. This reminds us that most β-phase BEDT-TTF salts are classified in L-mode structures.[2] Among a large variety of BEDT-TTF crystals, only a few exceptions which have two-fold ($\times 2$) lattices in the transverse directions are Z-mode crystals.

The present uniform structure is associated with the standing ethylthio parts, so it is surprising that even the C_1TMT-TTP salt has the same structure. This is probably because the methylthio unit strongly prefers uniform stacking, as many MDT-TSF salts form uniform columns. The preference for uniform stacks (and at the same time to the molecular mirror symmetry) decreases in the order of ethylthio (C_2T) > methylthio (C_1T) and similarly methylenedithio (MT) > ethylenedithio (ET). When we change these substituents, the crystal structure transforms successively from the Z-mode uniform, L-mode uniform to θ-type structures.

As for the electrical properties, the introduction of the MT unit instead of the ET unit reduces the electronic correlation, as the band width of the C_2TMT-TTP salt estimated from the thermoelectric power (1.2 eV) is larger than that of the ET analog (0.86 eV). By contrast, the introduction of the 1,3-dithiane unit in C_2TDA-TTP enhances the correlation; the resistivity of $(C_2TDA\text{-}TTP)_2PF_6$ is higher than those of the C_nTMT-TTP salts, and this compound shows an increase of resistivity below 15 K, though the origin of this upturn is uncertain. Furthermore, this donor gives entirely insulating salts such as $(C_2TDA\text{-}TTP)GaCl_4$ and $(C_2TDA\text{-}TTP)_2$(DMTCNQ). Thus we can say that the enhancement of correlation is successfully achieved by the introduction of the 1,3-dithiane unit, although we could not obtain an intermediate compound which undergoes a definite metal–insulator transition.

Experimental

General Data. Trimethyl phosphite was distilled under nitrogen by fractional distillation. Melting points were determined with a Yanaco MP micro melting point apparatus. NMR spectra were obtained with a JEOL JNM-AL300 spectrometer. Cyclic voltammetry spectra were measured on a Yanaco VMA-010 spectrometer. Microanalyses were performed at the Microanalytical Laboratory, Tokyo Institute of Technology. IR spectra were recorded on a SHIMADZU FTIR-8000 spectrometer.

C_2TMT-TTP (3). 4,5-bis(ethylthio)-1,3-dithiol-2-thione (**1**) 0.34 g (0.92 mmol) and **2** 0.70 g (2.75 mmol) in 15 mL trimethyl phosphite and 10 mL toluene were reacted at 115 °C for 3 h. After cooling, the resulting solids were collected, washed with methanol, and chromatographed (silica gel, CS_2) to give 47 mg of **3** (9% yield): a red solid. mp 186–188 °C. ^1H NMR ($CDCl_3$) δ 1.29–1.33 (t, 6H), 2.80–2.87 (m, 4H), 4.96 (s, 2H). Anal. Calcd for $C_{15}H_{12}S_{12}$: C, 31.22; H, 2.10; S, 66.68%. Found: C, 31.26; H, 2.10; S, 66.97%.

C_1TMT-TTP was prepared similarly.[8]

4,5-Bis(ethylthio)-1,3-dithiol-2-ylidene)-5-(1,3-dithian-2-yl)-1,3,4,6-tetrathiapentalene (5). 4,5-[(1,3-Dithian-2-yl)methylenedithio]-1,3-dithiol-2-one (**4**)[7,9] 40 mg (0.45 mmol) and **1** 228 mg (0.90 mmol) in 8 mL trimethylphosphite and 20 mL toluene were reacted at 110 °C for 5 h. After cooling, the resulting solids were collected, washed with hexane, and chromatographed (silica gel, CS_2) to give an orange solid (**5**) 76 mg (33% yield).

C_2TDA-TTP (6). To a 10 mL 1,1,2-trichloroethane solution of **5** 76 mg (0.146 mmol) was added DDQ 40 mg (0.175 mmol) dissolved in 20 mL 1,1,2-trichloroethane, and the resulting dark solution was heated at 130 °C for 2 h. The cooled reaction mixture was filtered, and the filtrate was concentrated under vacuum. The

residue was purified through silica-gel chromatography with CS_2 as an eluent, to give 54 mg (0.105 mmol) of **6** (71% yield). mp 146 °C. ^{1}H NMR ($CDCl_3$) δ 1.31 (t, $J = 7.2$ Hz, 6H), 2.20 (s, 2H), 2.81–2.91 (m, 8H). Anal. Calcd for $C_{15}H_{16}S_{10}$: C, 34.85; H, 3.12; S, 62.03%. Found: C, 34.90; H, 3.32; S, 62.09%.

X-ray Analysis. Single crystal data were measured by a Rigaku automated four-circle diffractometer AFC-7R with graphite monochromatized Mo Kα radiation ($\lambda = 0.71069$ Å). All measurements were performed at room temperature. The crystal structures were solved by the direct method, SIR-92.[19] The structures were refined by the full-matrix least-squares refinement. Crystallographic data have been deposited at the CCDC, 12 Union Road, Cambridge CB2 1EZ, UK and copies can be obtained on request, free of charge via http://www.ccdc.cam.ac.uk/conts/retrieving.html (or Fax: +44 1223 336033; e-mail: deposit@ccdc.cam.ac.uk), by quoting the publication citation and the deposition numbers CCDC 267828 and 267829.

Physical Properties. Electric resistivity was measured for a single crystal by the four-probe method using a low-frequency ac current. Electrical contacts to the crystals were made with 15 μm gold wire and carbon paint. The thermoelectric power was measured by attaching a sample to two copper blocks with pieces of gold foil and gold paint. The heat blocks were alternately heated with 2 min intervals at high temperatures, and the generated electromotive forces and the temperature gradients were measured. All measurements of transport properties were carried out along the crystal long axes, which correspond to the donor stacking axes.

The ESR spectra were measured with a JEOL JES-TE100 X-band spectrometer. The sample was mounted in such an orientation that the crystallographic *ac* plane is horizontal, and was rotated in this plane at room temperature (the inset in Fig. 6a). The temperature dependence was measured in the direction of *g* minimum, which is perpendicular to the donor planes.

This work was partly supported by a Grant-in-Aid for Scientific Research on Priority Areas of Molecular Conductors (No. 15073211) from the Ministry of Education, Culture, Sports, Science and Technology.

References

1 T. Ishiguro, K. Yamaji, and G. Saito, "Organic Superconductors," 2nd ed, Springer, Berlin (1998).

2 T. Mori, *Bull. Chem. Soc. Jpn.*, **71**, 2509 (1998); T. Mori, H. Mori, and S. Tanaka, *Bull. Chem. Soc. Jpn.*, **72**, 179 (1999); T. Mori, *Bull. Chem. Soc. Jpn.*, **72**, 2011 (1999).

3 Y. Misaki, H. Nishikawa, K. Kawakami, S. Koyanagi, T. Yamabe, and M. Shiro, *Chem. Lett.*, **1992**, 2321.

4 T. Mori, T. Kawamoto, Y. Misaki, K. Kawakami, H. Fujiwara, T. Yamabe, H. Mori, and S. Tanaka, *Mol. Cryst. Liq. Cryst.*, **284**, 271 (1996).

5 S. Kimura, H. Kurai, T. Mori, H. Mori, and S. Tanaka, *Bull. Chem. Soc. Jpn.*, **74**, 59 (2001); M. Aragaki, S. Kimura, M. Katsuhara, H. Kurai, and T. Mori, *Bull. Chem. Soc. Jpn.*, **74**, 833 (2001).

6 K. Takimuya, Y. Kataoka, Y. Aso, T. Otsubo, H. Fukuoka, and S. Yamanaka, *Angew. Chem., Int. Ed.*, **40**, 1122 (2001); K. Takimuya, M. Kodani, Y. Kataoka, Y. Aso, T. Otsubo, T. Kawamoto, and T. Mori, *Chem. Mater.*, **15**, 3250 (2003); K. Takimiya, A. Takamori, Y. Aso, T. Otsubo, T. Kawamoto, and T. Mori, *Chem. Mater.*, **15**, 1225 (2003); T. Kawamoto, T. Mori, K. Takimiya, A. Takamori, Y. Aso, and T. Otsubo, *Phys. Rev. B*, **65**, 140508 (2002); T. Kawamoto, T. Mori, C. Terakura, T. Terashima, S. Uji, K. Takimiya, Y. Aso, and T. Otsubo, *Phys. Rev. B*, **67**, 020508(R) (2003).

7 J. Yamada, M. Watanabe, H. Akutsu, S. Nakatsuji, H. Nishikawa, I. Ikemoto, and K. Kikuchi, *J. Am. Chem. Soc.*, **123**, 4174 (2001); J. Yamada, *J. Mater. Chem.*, **14**, 2951 (2004).

8 Y. Misaki, H. Nishikawa, T. Yamabe, T. Mori, H. Inokuchi, H. Mori, and S. Tanaka, *Chem. Lett.*, **1993**, 729.

9 J. Yamada, S. Satoki, S. Mishima, N. Akashi, K. Takahashi, N. Masuda, Y. Nishimoto, S. Takahashi, and H. Anzai, *J. Org. Chem.*, **61**, 3987 (1996); J. Yamada, N. Akashi, H. Anzai, M. Tamura, Y. Nishio, and K. Kajita, *Mol. Cryst. Liq. Cryst.*, **296**, 53 (1997); J. Yamada, *Recent Res. Dev. Org. Chem.*, **2**, 525 (1998).

10 J. Yamada, *Trends Org. Chem.*, **9**, 115 (2001); J. Yamada, T. Mangetsu, H. Akutsu, S. Nakatsuji, H. Nishikawa, I. Ikemoto, and K. Kikuchi, *Chem. Lett.*, **2001**, 86.

11 J. Yamada, S. Tanaka, J. Segawa, M. Hamasaki, K. Hagiya, H. Anzai, H. Nishikawa, I. Ikemoto, and K. Kikuchi, *J. Org. Chem.*, **63**, 3952 (1998).

12 J. Yamada, R. Oka, T. Mangetsu, H. Akutsu, S. Nakatsuji, H. Nishikawa, I. Ikemoto, and K. Kikuchi, *Chem. Mater.*, **13**, 1770 (2001).

13 T. Mori, H. Inokuchi, Y. Misaki, H. Nishikawa, T. Yamabe, H. Mori, and S. Tanaka, *Chem. Lett.*, **1993**, 733.

14 T. Mori, A. Kobayasi, Y. Sasaki, H. Kobayashi, G. Saito, and H. Inokuchi, *Bull. Chem. Soc. Jpn.*, **57**, 627 (1984).

15 J. Ouyang, K. Yakushi, Y. Misaki, and K. Tanaka, *J. Phys. Soc. Jpn.*, **67**, 3191 (2002); T. Kawamoto, M. Ashizawa, T. Mori, T. Yamamoto, J. Yamaura, and Y. Misaki, *J. Phys. Soc. Jpn.*, **71**, 3059 (2002); O. Drozdova, K. Yakushi, Y. Misaki, and K. Tanaka, *J. Solid State Commun.*, **168**, 497 (2002).

16 R. D. Barnard, "Thermoelectricity in Metals and Alloys," Taylor and Francis, London (1972); D. K. C. MacDonald, "Thermoelectricity: an Introduction to the Principles," Wiley, New York (1962).

17 T. Sugano, G. Saito, and M. Kinoshita, *Phys. Rev. B*, **35**, 6554 (1987).

18 G. Feher and A. F. Kip, *Phys. Rev.*, **98**, 337 (1955).

19 A. Altomare, M. Cascrano, C. Giacovazzo, and A. Guagiliardi, *J. Appl. Crystallogr.*, **26**, 343 (1993).